

DOI 10.24425/aee.2026.156804

# Abnormal noise detection of three-phase induction motor using linear predictive coding and neural networks

ADAM GLOWACZ<sup>1</sup>✉, MIROSLAW CZECHOWSKI<sup>2</sup>, FRANTISEK BRUMERIC<sup>3</sup>,  
MIROSLAV GUTTEN<sup>4</sup>, WITOLD GLOWACZ<sup>1</sup>

<sup>1</sup>AGH University of Krakow,

Faculty of Electrical Engineering, Automatics, Computer Science and Biomedical Engineering,  
Department of Automatic Control and Robotics,  
al. A. Mickiewicza 30, 30-059 Krakow, Poland

<sup>2</sup>Cracow University of Technology, CUT Doctoral School,  
Faculty of Electrical and Computer Engineering,  
ul. Warszawska 24, 31-155, Krakow, Poland

<sup>3</sup>University of Zilina,

Faculty of Mechanical Engineering, Department of Design and Machine Elements,  
Univerzitna 1, 010 26 Zilina, Slovakia

<sup>4</sup>University of Zilina,

Faculty of Electrical Engineering and Information Technology,  
Department of Mechatronics and Electronics,  
Univerzitna 1, 010 26 Zilina, Slovakia

e-mail: ✉ [adglow@agh.edu.pl](mailto:adglow@agh.edu.pl), [miroslaw.czechowski@doktorant.pk.edu.pl](mailto:miroslaw.czechowski@doktorant.pk.edu.pl), [brumeric1@uniza.sk](mailto:brumeric1@uniza.sk),  
[miroslav.gutten@uniza.sk](mailto:miroslav.gutten@uniza.sk), [wglowacz@agh.edu.pl](mailto:wglowacz@agh.edu.pl)

(Received: 29.06.2025, revised: 23.01.2026)

**Abstract:** The paper presents an abnormal noise detection method for a three-phase induction motor. The following motor conditions were analyzed: healthy (H), motor with one broken rotor bar (1BRB), motor with two broken rotor bars (2BRB), and motor with three broken rotor bars (3BRB). The dataset was split into 48 training samples (12 per class) and 168 test samples (42 per class) for the training and evaluation of the neural networks. Linear predictive coding (LPC) was used for feature extraction. The next three original neural networks were proposed for classification: Neural Network V01, V02, and V03. The authors of the paper also used ResNet-50. The proposed approach achieved a recognition efficiency of 100%.

**Key words:** acoustic, diagnosis, fault, neural network, noise



© 2026. The Author(s). This is an open-access article distributed under the terms of the Creative Commons Attribution-NonCommercial-NoDerivatives License (CC BY-NC-ND 4.0, <https://creativecommons.org/licenses/by-nc-nd/4.0/>), which permits use, distribution, and reproduction in any medium, provided that the Article is properly cited, the use is non-commercial, and no modifications or adaptations are made.

## 1. Introduction

Electric motor diagnostics are essential for safety and cost efficiency in industrial applications. Detection of electric motor faults, such as bearing wear, winding defects, misalignment, shorted rotor coils, and broken bars, can prevent costly breakdowns, extend motor lifespan, and reduce repair expenses. The fault diagnosis technique minimizes unplanned downtimes, keeping production lines running and avoiding financial losses. The fault diagnosis technique also reduces the risk of fires and equipment damage caused by motor failures. Fault diagnosis techniques provide financial savings, higher safety standards, and uninterrupted production.

## 2. Literature review on acoustic fault diagnosis

Existing literature includes numerous studies on acoustic-based fault diagnosis for electric motors [1–12]. Article [1] presented a fault diagnosis technique for three-phase induction motors using acoustic analysis. Acoustic signals for three conditions of the motors were analyzed: healthy, motor with two broken bars, and motor with a faulty ring of the squirrel cage. The models were trained on 60 one-second samples (20 per class) and tested on 180 (60 per class). The microphone was positioned parallel to the induction motor. The authors introduced an innovative feature extraction method called MoD-7 (maxima of differences between conditions). Neural networks, GoogLeNet, and ResNet-50 were used for classification. The computed results were very high, achieving a diagnostic accuracy of 100% across all three conditions.

Article [2] presented a method for diagnosing faults in commutator motors using acoustic data and a transfer learning approach. The method called high contrast frequency maps with lowpass filter (HCFMwLF) was proposed. The author of the paper analyzed the following states of the commutator motor: healthy, broken gear, broken gear tooth, broken fan, short-circuit in stator winding, and four drilled holes in the front bearing. The models were trained on 814 training samples and tested on 111. The K669B microphone was used. The study evaluated three deep learning architectures: GoogLeNet, ResNet-50, and VGG-19, achieving 100% efficiency of fault classification.

The next article proposed a novel approach to address the issue of mill fault diagnosis under limited datasets [3]. The proposed approach leveraged vibration and acoustic signal analysis to enhance diagnostic accuracy. Two experimental datasets were used, and the computed results showed high diagnostic performance despite data constraints. The models were trained on 146 samples and evaluated on 1314 samples.

A novel rolling bearing fault diagnosis method based on feature extraction and a word bag model was presented [4]. The experimental evaluation was conducted using 400 test samples. It used the adaptive extended bag-of-words model (AEBW). The approach showed high effectiveness, achieving a classification accuracy of 98.2% for five distinct fault types. This methodology presents a viable solution for mechanical equipment condition monitoring.

The next paper presented fan fault diagnosis using acoustic emission [5]. The original dataset of 120 samples was expanded to 840 through data augmentation. Three different microphone

positions were analyzed. The authors used a spectrogram and a convolutional neural network. The following conditions were analyzed: no-fault and fault. The accuracy of the proposed technique was equal to 0.95.

In another study, an acoustic fault diagnosis technique for rolling bearing faults was presented [6]. The proposed approach was based on Squeeze and Excitation ResNet (SE-ResNet). The computed accuracy for rolling bearing faults and SE-ResNet was equal to 99.02%.

The following paper proposed the use of the artificial fish swarm algorithm (AFSA) for rolling bearing fault diagnosis [7]. The method was based on the analysis of acoustic signals, and the results showed that it can effectively diagnose bearing faults.

The following article proposed a few-shot learning-based graph neural network model for the acoustic analysis of planetary gears in a wind turbine gearbox [8]. The dataset of 120 images (24 categories) was split into training (70 images, 14 categories), test (25 images, 5 categories), and validation (25 images, 5 categories) sets. The authors used the short-time Fourier transform (STFT) to preprocess the acoustic data. The proposed method achieved an accuracy of 98.69%.

The next method is based on analyzing the features of vibration and acoustic signals from an induction motor using a multi-input convolutional neural network [9]. Six operating conditions were analyzed for the bearing and gear. The accuracy of the proposed method was in the range of 93% to 100%.

A fault diagnosis technique for milling machines using acoustic signals was presented in [10]. A total of 400 samples were recorded, with 100 samples per investigated class. The following conditions were analyzed: bearing fault, gear fault, healthy state, and tool fault. A deep learning model optimized using a genetic algorithm was used for the analysis. The accuracy of the proposed methods was in the range of 91% to 100%.

The study introduces an acoustic-based framework for compound fault diagnosis. The proposed framework is based on an LP-LSGAN – a latent space-controlled generative adversarial network with a local perception mechanism [11]. The proposed method achieved a diagnostic accuracy of 93.49%.

A rolling bearing fault diagnosis method using vibro-acoustic data fusion is introduced [12]. The authors of the study used fast Fourier transform (FFT) and a convolutional neural network (CNN). The accuracy of the proposed method reaches 99.98%.

### 3. Acoustic measurements

Four similar three-phase induction motors (500 W) were analyzed. The following motor conditions were analyzed: healthy motor, motor with one broken rotor bar, motor with two broken rotor bars, and motor with three broken rotor bars (Fig. 1). The motors were mounted to the ground. The motors were arranged as shown in Figs. 1 and 2. The room was 7 meters by 5 meters. A Redmi Note 9 smartphone with a microphone, positioned 0.25 meters from each motor, captured the sound in AAC (advanced audio coding) format at a 48 kHz sampling rate, later converted to WAV (waveform audio file) format at 44.1 kHz for analysis. The use of a smartphone for measurements is justified by its ubiquity, cost-effectiveness, and sufficient technical capability for acoustic measurement.

Smartphones are equipped with high-quality microphones and processing power for capturing and storing acoustic signals. A smartphone can perform rapid and low-cost diagnostics.

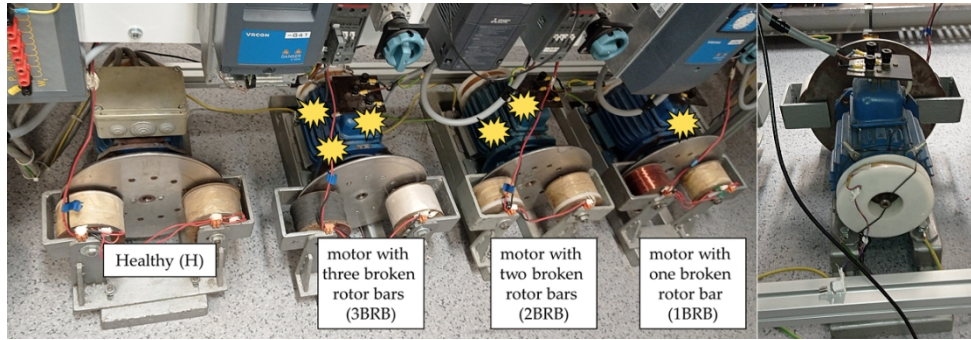


Fig. 1. Four similar three-phase induction motors (500 W)

The acoustic recording of the motor was performed in the room. The following tasks were taken to minimize ambient noise, such as closing windows and having no mechanical ventilation. Under these conditions, the sources of interference were reduced to reverberations and sound reflections from the walls. The detection method achieved a 100% recognition efficiency. It indicates that ambient factors were at an amplitude level sufficiently low not to overlap with the essential harmonic components of the motor acoustic signals.

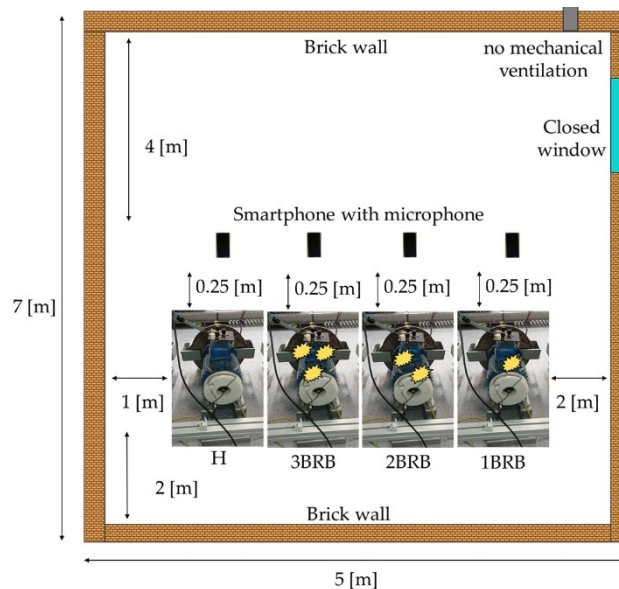


Fig. 2. Measurements of acoustic signals of three-phase induction motors

Acoustic signals of three-phase induction motors are presented in Fig. 3.

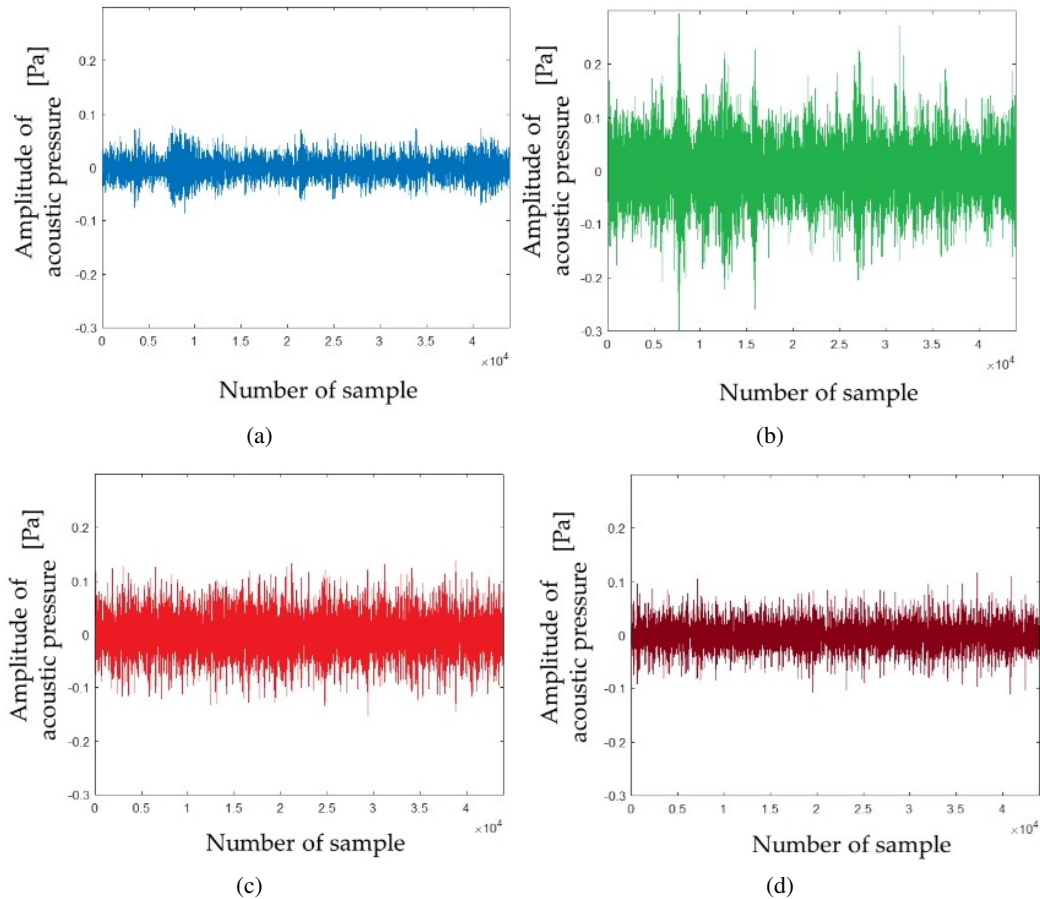


Fig. 3. Acoustic signals of three-phase induction motors: (a) healthy; (b) motor with one broken rotor bar; (c) motor with two broken rotor bars; (d) motor with three broken rotor bars

#### 4. Acoustic fault diagnosis method

The authors proposed an innovative diagnostic technique based on linear predictive coding (LPC) and neural networks V01, V02, and V03 (Fig. 4). First, the acoustic signal is recorded using a smartphone and saved in AAC format at a 48 kHz sampling rate. The signal is then converted into WAV (waveform audio file format) at 44.1 kHz for further processing. The recorded acoustic data are segmented into 1-second samples. 196 and 25 LPC coefficients are computed. Next, LPC coefficients are subsequently reshaped into acoustic images with dimensions of  $224 \times 224 \times 3$ . Three original neural networks are proposed and implemented: Neural Network V01, V02, and V03. The ResNet-50 neural network is also used for acoustic analysis.

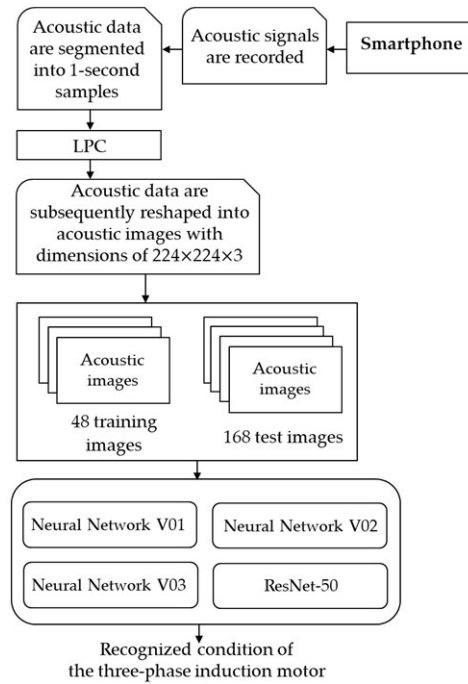


Fig. 4. Diagnostic technique based on linear predictive coding (LPC) and Neural Networks V01, V02, and V03

#### 4.1. Linear predictive coding

Linear predictive coding (LPC) is a method for compressing signals, speech, using modeling audio signals in the time domain. LPC assumes that the vocal tract can be represented by a filter. LPC is widely used in speech compression, speech synthesis, speech recognition, speaker identification, and speech signal analysis. LPC assumes that the current sample of a signal  $y(n)$  can be approximated as a linear combination of its previous samples. The current sample  $y(n)$  can be expressed as (1):

$$y(n) = \sum_{k=1}^p a_k \cdot y(n-k), \quad (1)$$

where:  $y(n)$  is the current sample,  $a_k$  is the LPC coefficient with the  $k$ -index,  $p$  is the prediction order.

The linear predictive coding determines the LPC coefficients that minimize the error between the actual sample and the predicted sample. The LPC coefficients can be achieved using methods such as the autocorrelation method or the covariance method. The advantages of LPC are its simplicity and good approximation of the vocal tract. The limitation of LPC is its sensitivity to background noise. A comprehensive discussion of LPC can be found in [13–15].

### 4.2. Acoustic images

The proposed neural networks require images with a resolution of  $224 \times 224 \times 3$ . The acoustic signals of an induction motor are first converted into LPC coefficients (196 coefficients in total, derived from the original 197 coefficients minus the first coefficient, and 25 coefficients, derived from the original 26 minus the first coefficient). These coefficients are then transformed into a  $14 \times 14$  matrix and a  $5 \times 5$  matrix. Next, the computed matrices are reshaped into the acoustic image with a target resolution of  $224 \times 224 \times 3$ . The computed  $14 \times 14$  acoustic images are shown in Fig. 5.

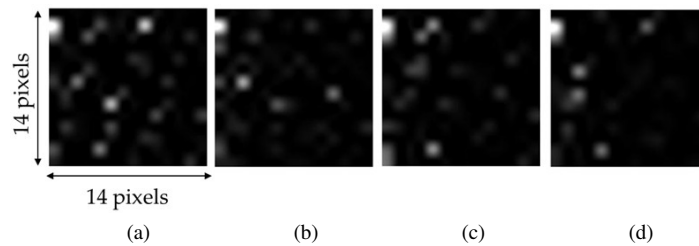


Fig. 5. Acoustic images of an induction motor ( $14 \times 14$  matrix representing 196 LPC coefficients): (a) healthy (H); (b) motor with one broken rotor bar (1BRB); (c) motor with two broken rotor bars (2BRB); (d) motor with three broken rotor bars (3BRB)

We can see that the LPC coefficients are different for the four acoustic signals of the induction motor. These computed acoustic images serve as inputs for the proposed Neural Networks (V01, V02, and V03). There are also other types of neural networks described in the literature [16–18].

### 4.3. Neural Network V01

Neural Network V01 is a small neural network designed for image recognition. The required input images must have a resolution of  $224 \times 224 \times 3$ . The Neural Network V01 consists of 8 blocks and is illustrated in Fig. 6.

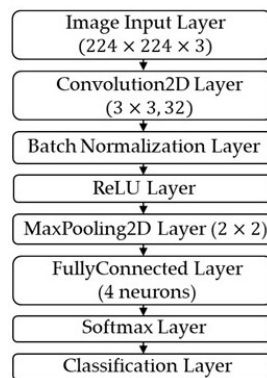


Fig. 6. Structure of Neural Network V01

#### 4.4. Neural Network V02

Neural Network V02 is also a neural network designed for image recognition. The input images must have a resolution of  $224 \times 224 \times 3$ . It is similar to Neural Network V01. The Neural Network V02 is presented in Fig. 7. Additional layers have been added, including: Convolution2D Layer ( $3 \times 3, 32$ ), Batch Normalization Layer, ReLU Layer, MaxPooling2D Layer, and FullyConnected Layer (32). The layers in Neural Network V02 are connected sequentially.

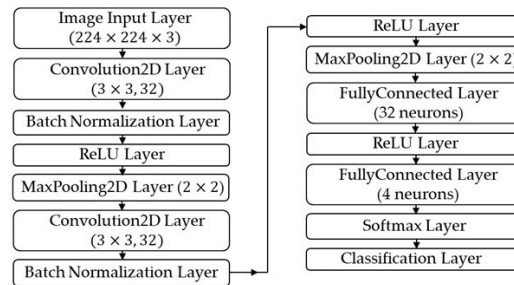


Fig. 7. Structure of Neural Network V02

#### 4.5. Neural Network V03

Neural Network V03 is a neural network designed for image recognition. Its image input layer requires images in  $224 \times 224 \times 3$  format. The Neural Network V03 is shown in Fig. 8. The architecture of Neural Network V03 is illustrated in Fig. 8 and includes the following additional

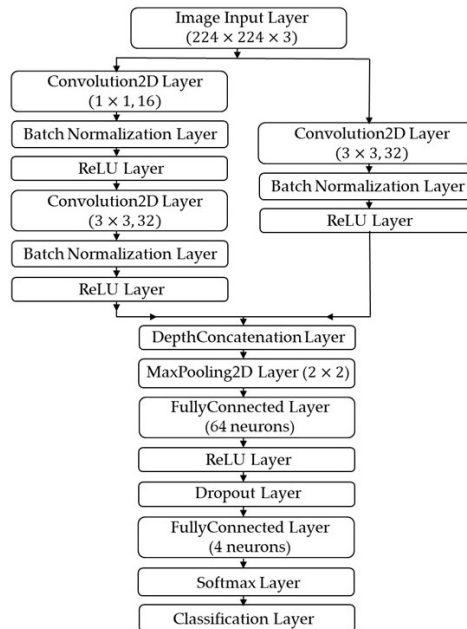


Fig. 8. Structure of Neural Network V03

layers: Convolution2D Layer ( $1 \times 1, 16$ ), Convolution2D Layer ( $3 \times 3, 32$ ), FullyConnected Layer (64), Batch Normalization Layer, and DepthConcatenation Layer. The layers in the V03 Neural Network are connected in parallel, enabling more complex feature processing.

#### 4.6. ResNet-50

ResNet-50 is a convolutional neural network. It was introduced in 2015 to solve the vanishing gradient problem using residual blocks. It allows gradients to flow directly by adding input to deeper layers. It enables stable training. ResNet-50 also uses bottleneck blocks ( $1 \times 1, 3 \times 3, 1 \times 1$  convolutions) to reduce computational complexity. It achieved very good results for object detection. It is an efficient neural network using residual blocks. Further details can be found in the literature [19–25].

### 5. Acoustic analysis of the three-phase induction motor

Acoustic analysis was performed on four induction motors with the following conditions: healthy (H), motor with one broken rotor bar (1BRB), motor with two broken rotor bars (2BRB), and motor with three broken rotor bars (3BRB). The authors used 48 training samples (12 training samples per class) to train the neural networks. The authors used 168 test samples (42 test samples per class) to test the neural networks.  $K$ -fold cross-validation was applied in the acoustic analysis. Recognition efficiency ( $E_R$ ) was computed as follows (2):

$$E_R = 100\% * (\text{RecognizedTestSamples} / \text{OneClassTestSamples}), \quad (2)$$

where: RecognizedTestSamples – correctly identified test samples, OneClassTestSamples – test samples per class (42 test samples in the study).

Table 1 presents the acoustic analysis results of the three-phase induction motor using LPC (196 coefficients), and the following neural networks: Neural Network V01, V02, V03, and ResNet-50.

Table 1. Acoustic analysis results of the three-phase induction motor using LPC (196 coefficients), and Neural Network V01, V02, V03, and ResNet-50

Condition of the motor	$E_R$ [%]			
	ResNet-50	Neural Network V01	Neural Network V02	Neural Network V03
$E_{R1}$ , healthy (H)	100	100	100	100
$E_{R2}$ , (1BRB)	100	100	100	100
$E_{R3}$ , (2BRB)	100	100	100	100
$E_{R4}$ , (3BRB)	100	100	100	100

Table 2 presents the acoustic analysis results of the three-phase induction motor using LPC (25 coefficients), and the following neural networks: Neural Network V01, V02, V03, and ResNet-50.

Table 2. Acoustic analysis results of the three-phase induction motor using LPC (25 coefficients), and Neural Network V01, V02, V03, and ResNet-50

Condition of the motor	$E_R$ [%]			
	ResNet-50	Neural Network V01	Neural Network V02	Neural Network V03
$E_{R1}$ , healthy (H)	100	100	100	97.6
$E_{R2}$ , (1BRB)	100	100	100	100
$E_{R3}$ , (2BRB)	100	100	100	100
$E_{R4}$ , (3BRB)	100	100	100	100

Confusion matrices for neural networks are presented in Figs. 9, 10, 11.

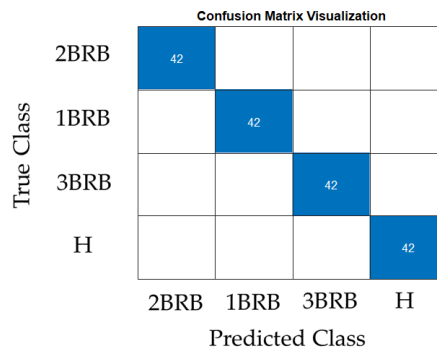


Fig. 9. Visualization of the confusion matrix for the V01, V02, ResNet-50 Neural Networks (196 and 25 LPC coefficients)

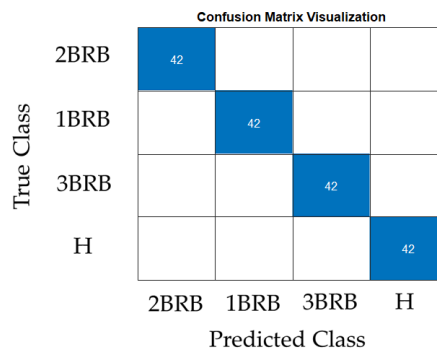


Fig. 10. Visualization of the confusion matrix for Neural Network V03 (196 LPC coefficients)

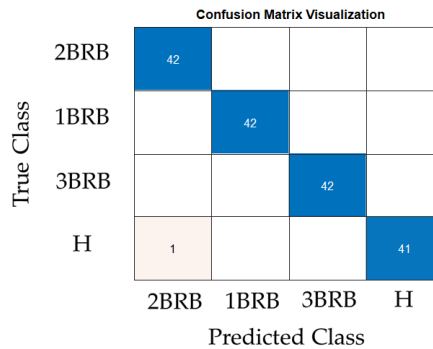


Fig. 11. Visualization of the confusion matrix for Neural Network V03 (25 LPC coefficients)

The results of the acoustic analysis are presented in Tables 1 and 2. The proposed LPC-based approach, combined with neural networks, offered an effective fault diagnosis for three-phase induction motors. This methodology shows potential for diagnosing other motor types and fault conditions when combined with LPC and neural network techniques.

## 6. Discussion

The developed approach has high recognition efficiency ( $E_R = 100\%$ ) for detecting faults of the induction motor. Computed results are competitive with those in the literature [1]. Several diagnostic approaches exist for induction motor condition monitoring: acoustic-based, vibration-based, electrical signal analysis, and thermography. Acoustic-based methods utilize sound wave analysis to detect various faults, including bearing defects, air gap irregularities, and certain electrical faults. Advantages of acoustic-based methods are non-invasive measurement and potential for early fault detection. However, disadvantages are particularly susceptible to environmental noise and signal distortions [2]. Vibration-based methods use accelerometers. These methods are efficient for detecting mechanical faults in induction motors, such as misalignment and bearing wear. However, they are less effective for electrical faults. Electrical signal analysis, particularly motor current signature analysis (MCSA), effectively detects stator and rotor faults by monitoring current signatures [26]. Electrical signal analysis is particularly effective for identifying rotor and stator winding defects, air gap eccentricity, and supply voltage imbalances. Thermal analysis serves as a valuable diagnostic tool for identifying thermal anomalies in induction motors, including broken rotor bar faults, winding insulation degradation, and bearing lubrication failures [27]. The advantage of thermal analysis is that it is a non-invasive measurement. The next advantage is visual fault representation through thermal maps and detecting developing faults before failure. However, a dirty motor can be difficult to diagnose. Thermal analysis can be difficult for changes in thermal radiation from the environment, e.g., 100 electric motors in the same room. While each method has strengths, combining acoustics, vibrations, and electrical analysis provides the most comprehensive fault coverage. Thermal analysis can serve as a supplementary tool for thermal monitoring.

## 7. Conclusions

The abnormal noise detection method for a three-phase induction motor is presented in the paper. The following motor conditions were analyzed: healthy motor, motor with one broken rotor bar, motor with two broken rotor bars, and motor with three broken rotor bars. Four similar three-phase induction motors were analyzed. The authors used linear predictive coding for feature extraction. Three original neural networks were proposed and implemented: Neural Network V01, V02, and V03. The ResNet-50 neural network was also used for acoustic analysis.

The proposed approach correctly identified all faults. Broken motor rotor bars can be detected using the proposed approach. Acoustic fault diagnosis has potential applications in various industries, such as mining, oil, robotics, aviation, and automotive sectors. Implementing fault diagnosis for industrial motors could lead to significant cost savings.

Future research will focus on developing new diagnostic methods that utilize multiple signals, including acoustic and electric data. The proposed fault diagnosis techniques are expected to benefit both society and industry.

### Acknowledgements

The research was financed by a research subsidy from the Ministry of Education and Science of the Republic of Poland for the AGH University of Krakow.

### References

- [1] Glowacz A., Sulowicz M., Kozik J., Piech K., Glowacz W., Li Z.X., Brumerick F., Gutten M., Korenciak D., Kumar A., Lucas G.B., Irfan M., Caesarendra W., Liu H., *Fault diagnosis of electrical faults of three-phase induction motors using acoustic analysis*, Bulletin of the Polish Academy of Sciences Technical Sciences, vol. 72, no. 1 (2024), DOI: [10.24425/bpasts.2024.148440](https://doi.org/10.24425/bpasts.2024.148440).
- [2] Zastepa M., *Commutator motor fault diagnosis using acoustic data with a transfer learning approach*, Przegląd Elektrotechniczny, vol. 100, no. 12, pp. 173–180 (2024), DOI: [10.15199/48.2024.12.40](https://doi.org/10.15199/48.2024.12.40).
- [3] He J.J., Shi P.M., Xu X.F., Han D.Y., *Rolling mill fault diagnosis under limited datasets*, Knowledge-Based Systems, vol. 291 (2024), DOI: [10.1016/j.knsys.2024.111579](https://doi.org/10.1016/j.knsys.2024.111579).
- [4] Guo X.W., *Fault Diagnosis of Rolling Bearings Based on Acoustics and Vibration Engineering*, IEEE Access, vol. 12, pp. 139632–139648 (2024), DOI: [10.1109/ACCESS.2024.3466154](https://doi.org/10.1109/ACCESS.2024.3466154).
- [5] Ciaburro G., Padmanabhan S., Maleh Y., Puyana-Romero V., *Fan Fault Diagnosis Using Acoustic Emission and Deep Learning Methods*, Informatics-Basel, vol. 10, no. 1 (2023), DOI: [10.3390/informatics10010024](https://doi.org/10.3390/informatics10010024).
- [6] Gu X.J., Tian Y., Li C., Wei Y.H., Li D.S., *Improved SE-ResNet Acoustic-Vibration Fusion for Rolling Bearing Composite Fault Diagnosis*, Applied Sciences-Basel, vol. 14, no. 5 (2024), DOI: [10.3390/app14052182](https://doi.org/10.3390/app14052182).
- [7] Yan J., Zhou F.B., Zhu X., Zhang D.P., *AFSA-FastICA-CEEMD Rolling Bearing Fault Diagnosis Method Based on Acoustic Signals*, Mathematics, vol. 13, no. 5 (2025), DOI: [10.3390/math13050884](https://doi.org/10.3390/math13050884).
- [8] Yang S., Xu H.F., Wang Y., Chen J.H., Li C., *Fault diagnosis of wind turbine with few-shot learning based on acoustic signal*, Engineering Research Express, vol. 7, no. 1 (2025), DOI: [10.1088/2631-8695/ada5ac](https://doi.org/10.1088/2631-8695/ada5ac).
- [9] Choudhary A., Mishra R.K., Fatima S., Panigrahi B.K., *Multi-input CNN based vibro-acoustic fusion for accurate fault diagnosis of induction motor*, Engineering Applications of Artificial Intelligence, vol. 120 (2023), DOI: [10.1016/j.engappai.2023.105872](https://doi.org/10.1016/j.engappai.2023.105872).

- [10] Umar M., Siddique M.F., Ullah N., Kim J.M., *Milling Machine Fault Diagnosis Using Acoustic Emission and Hybrid Deep Learning with Feature Optimization*, Applied Sciences-Basel, vol. 14, no. 22 (2024), DOI: [10.3390/app142210404](https://doi.org/10.3390/app142210404).
- [11] Tu F.M., Zhang T.L., Liu T., Zhang D.C., Yang S.X., *A Novel Acoustic-Based Framework for Compound Fault Diagnosis in Rotating Machinery with Limited Samples*, IEEE Transactions on Instrumentation and Measurement, vol. 74 (2025), DOI: [10.1109/TIM.2025.3551919](https://doi.org/10.1109/TIM.2025.3551919).
- [12] Fang X., Zheng J.B., Jiang B., *A rolling bearing fault diagnosis method based on vibro-acoustic data fusion and fast Fourier transform (FFT)*, International Journal of Data Science and Analytics (2024), DOI: [10.1007/s41060-024-00609-7](https://doi.org/10.1007/s41060-024-00609-7).
- [13] Mohammad M., Ibryaeva O., Sinitin V., Ereemeeva V., *A Computationally Efficient Method for the Diagnosis of Defects in Rolling Bearings Based on Linear Predictive Coding*, Algorithms, vol. 18, no. 2 (2025), DOI: [10.3390/a18020058](https://doi.org/10.3390/a18020058).
- [14] Ashraf F.F., Mobeen S., Khan H.Z.I., Haydar M.F., Riaz J., *Detection of Oscillatory Failures in Hydraulic Actuators of Aircraft using Linear Predictive Coding and Signal Spectrum Analysis*, IFAC PapersOnLine, vol. 56, no. 2, pp. 360–365 (2023), DOI: [10.1016/j.ifacol.2023.10.1594](https://doi.org/10.1016/j.ifacol.2023.10.1594).
- [15] Gong C.S.A., Su C.H.S., Liu Y.E., Guu D.Y., Chen Y.H., *Deep Learning with LPC and Wavelet Algorithms for Driving Fault Diagnosis*, Sensors, vol. 22, no. 18 (2022), DOI: [10.3390/s22187072](https://doi.org/10.3390/s22187072).
- [16] Kirda A.W., Majewski P., Bursy G., Bartoszek M., Yassin H., Królczyk G., Akbar N.A., Caesarendra W., *Integrating YOLOv5, Jetson nano microprocessor, and Mitsubishi robot manipulator for real-time machine vision application in manufacturing: A lab experimental study*, Advances in Science and Technology Research Journal, vol. 19, no. 5, pp. 248–270 (2025), DOI: [10.12913/22998624/201366](https://doi.org/10.12913/22998624/201366).
- [17] Gajewski J., Valis D., *Verification of the technical equipment degradation method using a hybrid reinforcement learning trees-artificial neural network system*, Tribology International, vol. 153 (2021), DOI: [10.1016/j.triboint.2020.106618](https://doi.org/10.1016/j.triboint.2020.106618).
- [18] Jiang K.S., Zhang C.S., Wei B.L., Li Z.X., Kochan O., *Fault diagnosis of RV reducer based on denoising time-frequency attention neural network*, Expert Systems with Applications, vol. 238 (2024), DOI: [10.1016/j.eswa.2023.121762](https://doi.org/10.1016/j.eswa.2023.121762).
- [19] Zhang L.Y., Bian Y.C., Jiang P., Zhang F.Y., *A Transfer Residual Neural Network Based on ResNet-50 for Detection of Steel Surface Defects*, Applied Sciences-Basel, vol. 13, no. 9 (2023), DOI: [10.3390/app13095260](https://doi.org/10.3390/app13095260).
- [20] Wen L., Xiao Z.K., Xu X.T., Liu B., *Disaster Recognition and Classification Based on Improved ResNet-50 Neural Network*, Applied Sciences-Basel, vol. 15, no. 9 (2025), DOI: [10.3390/app15095143](https://doi.org/10.3390/app15095143).
- [21] Jeong M., Yang M., Jeong J., *Hybrid-DC: A Hybrid Framework Using ResNet-50 and Vision Transformer for Steel Surface Defect Classification in the Rolling Process*, Electronics, vol. 13, no. 22 (2024), DOI: [10.3390/electronics13224467](https://doi.org/10.3390/electronics13224467).
- [22] Wu D.H., Ying Y.B., Zhou M.C., Pan J.M., Cui D., *Improved ResNet-50 deep learning algorithm for identifying chicken gender*, Computers and Electronics in Agriculture, vol. 205 (2023), DOI: [10.1016/j.compag.2023.107622](https://doi.org/10.1016/j.compag.2023.107622).
- [23] Sahin M.E., Ulutas H., Yuce E., Erkoç M.F., *Detection and classification of COVID-19 by using faster R-CNN and mask R-CNN on CT images*, Neural Computing & Applications, vol. 35, no. 18, pp. 13597–13611 (2023), DOI: [10.1007/s00521-023-08450-y](https://doi.org/10.1007/s00521-023-08450-y).
- [24] Patil R.A., Dixit V.V., *Detection and classification of mammogram using ResNet-50*, Multimedia Tools and Application (2025), DOI: [10.1007/s11042-025-20679-4](https://doi.org/10.1007/s11042-025-20679-4).
- [25] Panda M.K., Subudhi B.N., Thangaraj V., Jakhetiya V., *Two streams ResNet-50 network for infrared and visible image fusion*, Multimedia Tools and Application (2025), DOI: [10.1007/s11042-025-20869-0](https://doi.org/10.1007/s11042-025-20869-0).

- [26] Bessous N., Sbaa S., Megherbi A.C., *Mechanical fault detection in rotating electrical machines using MCSA-FFT and MCSA-DWT techniques*, Bulletin of the Polish Academy of Sciences Technical Sciences, vol. 67, no. 3, pp. 571–582 (2019), DOI: [10.24425/bpasts.2019.129655](https://doi.org/10.24425/bpasts.2019.129655).
- [27] Sasithradevi A., Persiya J., Roomi S.M.M., Perumal D.A., Prakash P., Vijayalakshmi M., Ebenezer LB., *Advanced thermal vision techniques for enhanced fault diagnosis in electrical equipment: a review*, International Journal of System Assurance Engineering and Management, vol. 16, no. 5, pp. 1914–1932 (2025), DOI: [10.1007/s13198-025-02782-9](https://doi.org/10.1007/s13198-025-02782-9).